In-nozzle flow and spray characteristics of large two-stroke marine diesel fuel injectors

Applied Thermal Engineering 180 (2020) 115809

Contents lists available at ScienceDirect

Applied Thermal Engineering

journal homepage: www.elsevier.com/locate/apthermeng

In-nozzle flow and spray characteristics of large two-stroke marine diesel fuel injectors

Reto Balz[a,b,*], Beat von Rotz[b], David Sedarsky[a]

[a] Department of Mechanics and Maritime Sciences, Chalmers University of Technology, Hörsalsvägen 7A, 412 58 Göteborg, Sweden
[b] Winterthur Gas & Diesel Ltd., Sulzer Allee 19, CH-8404 Winterthur, Switzerland

HIGHLIGHTS

- An eccentric low-speed marine engine fuel injector nozzle design was investigated.
- In-nozzle flow cavitation was confirmed by visualization via transparent nozzle.
- Swirl cavitation pattern affecting spray morphology/formation shown.
- Hydro-erosive grinding does not completely remove in-nozzle cavitation flow.

ARTICLE INFO

Keywords:
In-nozzle flow
Cavitation
Spray
Marine Diesel engine
Fuel injection

MSC 2020:
00-01
99-00

ABSTRACT

To further increase efficiency as well as to reduce emissions of large two-stroke marine Diesel engines, the understanding of the fuel injection processes and the resulting spray atomization characteristics is of high importance. The sheer dimensions, the uniflow scavenging design with the central exhaust valve position and the high swirl motion of the charge air is imposing the need for peripheral multiple fuel injector arrangement. The two or three fuel injectors are arranged by 180° resp. 120° and hence, a strongly asymmetrical and eccentrical atomizer design is given as all of the typically five orifices face a similar direction which is defined by the injector position and swirl flow. Experiments have shown that these characteristic nozzle tip bore arrangements lead to a strong spray deflection due to inhomogeneous velocity profiles induced by cavitation inside the orifice. Specifically designed transparent nozzles have been utilized to qualitatively investigate the in-nozzle cavitation flow phenomena. Furthermore, the influence on the subsequent atomization behaviour by simultaneously acquiring the spray morphology has been studied. A simplified transparent one-hole nozzle was used with a matching nozzle tip geometry representative for a large two-stroke marine Diesel engine injector. Fuel pressures of 50 MPa were applied to meet engine realistic injection conditions. Moreover, different degrees of hydro-erosive grinding were applied to the orifices to investigate the effects on the spray morphology with decreasing levels of in-nozzle flow cavitation derived by increasing inlet radii between main nozzle tip bore and orifice.

1. Introduction

Large two-stroke marine Diesel engines are widely used to propel commercial ships like tankers, bulk carriers as well as container and cargo vessels. Most of the traded goods in the world are transported by sea as it remains the most efficient means of transportation [1]. To further increase efficiency and lower emissions, understanding of the spray formation and its antecedent fuel injection is of high importance [2–4]. Fuel injector atomizers of large two-stroke marine Diesel engines have a highly complicated design due to a peripheral multi-injector arrangement and a strong swirl motion in the cylinder. The two or three fuel injectors are arranged by 180° resp. 120° around the central exhaust valve in the cylinder head. A typical injector nozzle tip has five different orifices which all face in a similar direction to provide sprays following the strong swirl motion to ensure efficient combustion. The nozzle bores have slightly different diameters, horizontal and vertical angles and eccentricities. A typical fuel injector of large two-stroke marine Diesel engines is depicted in Fig. 1 together with a detail of the nozzle tip and its five nozzle bore design. Previous experimental investigations and CFD simulations at Winterthur Gas & Diesel Ltd. (WinGD) have shown that the spray formation in large two-stroke marine Diesel engines is affected by the fuel injector in-nozzle flow due

* Corresponding author at: Winterthur Gas & Diesel Ltd., Sulzer Allee 19, CH-8404 Winterthur, Switzerland.
E-mail address: reto.balz@wingd.com (R. Balz).

https://doi.org/10.1016/j.applthermaleng.2020.115809
Received 12 May 2020; Received in revised form 24 June 2020; Accepted 24 July 2020
Available online 05 August 2020
1359-4311/

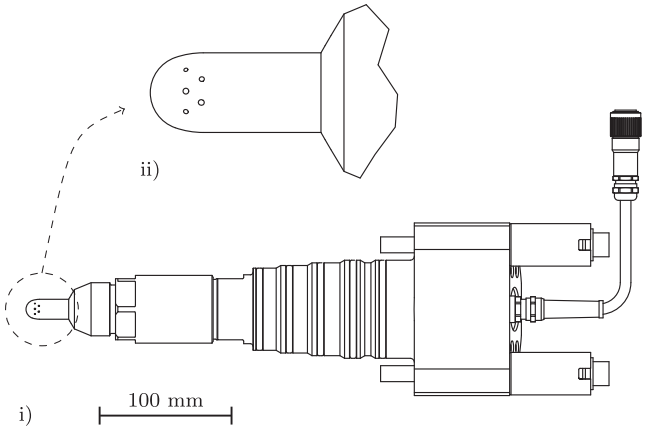

Fig. 1. Schematic illustration of a standard common rail fuel injector with mounted nozzle tip (i) as used in large two-stroke marine Diesel engines and enlarged (scale 4:1) detail of the nozzle tip with its five orifices (ii).

to inhomogeneous velocity profiles originating from cavitation effects [5–7]. These cavitation characteristics can lead to significant influences on the atomization process such as spray deflections in eccentric nozzles [8]. When not considered, this reduces engine efficiency and increases emissions due to fuel spray interactions with the cylinder wall and/or resulting changes in predicted combustion.

The fuel injection process in modern Diesel engines is based on high rail pressures and small nozzle bore diameters to enhance the spray atomization. This conditions however, lead to cavitation in the fuel injector and nozzles [9,10]. Various experimental as well as CFD studies have shown that cavitation in the nozzle bore enhances the spray breakup [11–15,10]. However, the undesirable effects of cavitation like flow instabilities, excessive noise generation and erosion that can cause damage to the injector components require detailed understanding of the complex phenomena [16].

Various experimental and numerical studies on cavitation characteristics for fuel injectors are available. Optically transparent nozzles with identical or scaled geometries allow for experimental in-nozzle flow visualization and enable characterizing cavitation. Limiting factors of such devices are high fuel pressures and the refractive index matching of the fuel and optical material [17]. Lately, a number of interesting experimental cavitation investigations with transparent nozzles, scaled and original-sized, at low pressures and towards more realistic pressures have been reported [18,19,17,20–23]. Kim and Park provide a current overview of transparent nozzle experiments summarizing the measurement technique, fuel, temperature and pressure conditions [24]. Unfortunately, most studies are focused on automotive fuel injectors with limited fuel pressures and scaled nozzles and are hardly relevant to large two-stroke marine Diesel engine fuel injector parameters, especially regarding the eccentric nozzle design. As a consequence, a transparent nozzle holder has been developed based on [17] to match the conditions of large two-stroke marine Diesel engines. Using realistic nozzle geometries and fuel pressures, the visualization of the in-nozzle flow cavitation is very close to the conditions found in large two-stroke marine Diesel engine fuel injection systems. Simultaneous spray morphology measurements were used to further deepen the understanding of how in-nozzle flow cavitation affects the spray breakup and to generate valuable validation data for design tools as well as CFD simulations. The gathered data helps to further deepen the understanding of the combustion process in the large two-stroke marine Diesel engine and consequently improves thermal efficiency and emissions.

2. Experimental setup

2.1. Transparent nozzles

A specially designed nozzle holder has been used to apply defined forces on all sides of the cuboid transparent nozzles made of polymethyl methacrylate (PMMA). This installation enables a homogeneous compression of the nozzles allowing for pressurization with engine realistic rail pressures of 50–80 MPa, typically applied in large two-stroke marine Diesel engines injection systems. The original nozzle tips usually have a five-hole configuration with the bores being eccentrically arranged with respect to the symmetrical axis of the nozzle tip main bore. However, the transparent nozzles are designed with a single orifice for simplification reasons regarding optical access, control of the hydro-erosive grinding process as well as reduced complexity and computational costs for CFD validations. Nevertheless, the geometrical design of the atomizer section is identical as found in large two-stroke marine Diesel engine fuel injectors. Since previous research work indicated strong spray deflections with eccentrical orifices, the geometry chosen for this study is a 0.8 mm eccentrically arranged nozzle bore with respect to the 3.5 mm main atomizer bore. The nozzle bore diameter is 0.75 mm. Fig. 2 shows a detailed illustration of the nozzle geometry used. PMMA as transparent material has been selected as it has an almost identical refractive index as Diesel fuel allowing for visualization of the in-nozzle flow without optical distortions due to the cylindrical nozzle bore that otherwise would behave like a convex lens and refract the light away from the optical axis. An alternative material would be fused silica glass (SiO_2) which has a similar refractive index as well, but showed not to be as pressure resistant as PMMA [19]. An additional advantage of PMMA is the more cost-efficient machining of the plastic compared to the glass.

The transparent PMMA nozzles are mounted in a transparent nozzle holder (TNH) [25] which also has a pressure sensor mounted at the end of the nozzle main bore and is depicted in a schematic in Fig. 3. The TNH can be mounted directly on the fuel injector using the injector mount (7). The side clamps (2) apply force on the transparent PMMA nozzle (4) via two sapphire bricks (3) that are polished on both sides to maintain optical access while the top clamps (5) apply force directly on the transparent nozzle. The main body (6) and sensor body apply force on the remaining two surfaces of the transparent nozzle cuboid by using two positioning bolts. The TNH is designed to match the geometrical properties of fuel injectors nozzles representative for large two-stroke marine Diesel engines. The installed pressure sensor (1) is a piezo-resistive, absolute sensor from Kistler (4067C2000) that allows for highly accurate pressure measurements of the involved phenomena. Together with a high data acquisition rate, detailed comparisons of different nozzle geometries are possible and accurate boundary conditions for CFD simulations can be generated. Furthermore, the pressure

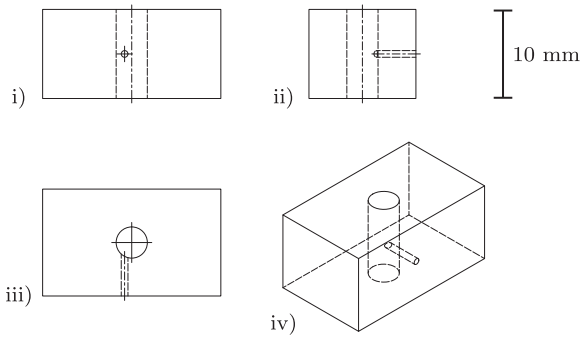

Fig. 2. Technical drawing of eccentric nozzle geometry used in this study with front (i), side (ii) and top view (iii), as well as an isometric view (iv). The main bore diameter is 3.5 mm, the nozzle bore diameter 0.75 mm and the eccentricity 0.8 mm.

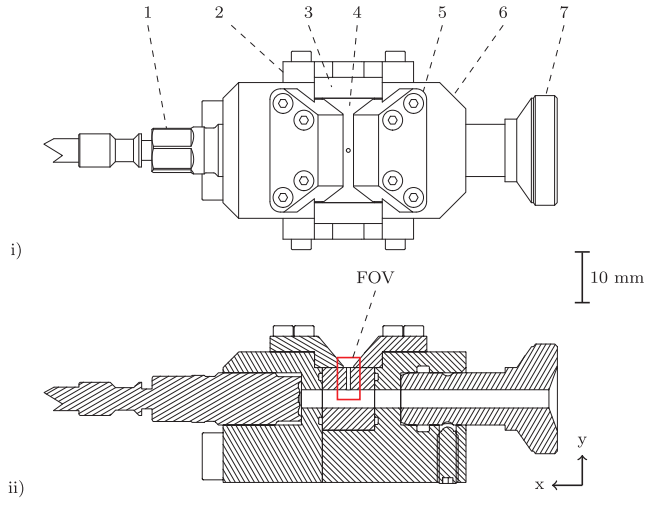

Fig. 3. Schematic illustration of transparent nozzle holder (TNH) with mounted PMMA nozzle. Top view (i) and sectional side view (ii) with pressure sensor (1), side clamp (2), sapphire brick (3), transparent PMMA nozzle (4), top clamp (5), main body (6) and injector mount (7). The red rectangle in the sectional side view (ii) indicates the field of view (FOV) used for the in-nozzle flow visualization. (For interpretation of the references to colour in this figure legend, the reader is referred to the web version of this article.)

measurement at the TNH is important since fuel injectors usually have a certain pressure drop across the injection valve. The TNH is described in more detail in [25,26].

2.2. Hydro-erosive grinding

An option to reduce cavitation in the orifices is to remove the sharp edge between main bore and orifice and hence, optimize flow. In commercially produced metallic fuel atomizer, this process is usually performed using electro-chemical machining, where a electrolyte is pumped through the nozzle tip and removes metal ions due to a set potential difference. As the nozzle tip has to be an electrical conductor for this process to be working, it is not applicable for the transparent PMMA nozzles used in this study. The alternative process is called hydro-erosive grinding and utilizes a non-Newtonian fluid with small abrasive particles that is pushed through the nozzle tips. The highly viscous fluid applies shear forces which allow the abrasive particles to remove material. In the test rig constructed to hydro-erosive grind the nozzles, the fluid is pressurized using a standard hydraulic system. A piston is moved in a cylinder that pushes the abrasive fluid through the nozzle tip using a special mount made for the PMMA nozzles. The system is controlled by a time based control unit. The hydraulic pressure of the system defines the velocity of the fluid flowing through the nozzle tip and therefore, also the rate of material removal. The hydro-erosive grinding fluid achieves highly repeatable results due to a homogeneous mixture of the fluid and particles and the relatively long grinding times at low pressure. The working fluid is a commercially available product from Gradnings & Maskinteknik AB (EM-70760-W/120S) and has been forced through the nozzles with a differential pressure of 1.5 MPa. The set duration for the hydro-erosive grinding of the transparent PMMA nozzles can be found in Table 1 together with the resulting nozzle bore exit diameters and evaluated inlet radii. Note that due to the pronounced level of hydro-erosive grinding of the nozzles, a complex, flow optimized geometry is generated which consists of multiple interconnected radii that lead to tapered and oval shaped nozzle bores. Hence, the provided radius in Table 1 serves only as rough approximation. To quantitatively characterize the hydro-erosive grinding process, the atomizers were analyzed using a nozzle-flow test rig at WinGD, that allows measuring the mass flow using a calibration oil with a pressure of 5 MPa. Tests have been performed where discharge coefficients of the nozzle tips were evaluated and no significant differences between identically hydro-erosive ground nozzle tips were found. The measured mass flows and the evaluated discharge coefficients of the six differently hydro-erosive ground nozzle tips are shown in Table 1.

Table 1
Properties of the six differently hydro-erosive ground nozzles used in this study.

nozzle number		i	ii	iii	iv	v	vi
hydro-erosive grinding time	[s]	0	60	120	180	240	300
nozzle bore exit diameter	[mm]	0.75	0.76	0.77	0.80	0.86	0.92
inlet radius	[mm]	0	0.08	0.16	0.37	0.56	0.69
mass flow at 5 MPa	[g/s]	19.9	25.3	28.8	30.7	32.8	36.4
discharge coefficient	[–]	0.49	0.62	0.71	0.75	0.81	0.89

2.3. Test facility

The experiments were performed in the constant volume Spray and Combustion Chamber (SCC) at WinGD in Winterthur, Switzerland. The SCC represents the combustion chamber of a 50 cm cylinder bore engine at TDC. Engine relevant conditions regarding pressure, temperature and swirl velocity can be achieved. More information on the test facility can be found in [27,28]. Due to the temperature limits of approximately 80 °C [17,29] of the PMMA nozzle tips used, the experiments were conducted under ambient gas temperature and back-pressure conditions. Previous experiments using the transparent nozzles with the TNH have shown that the back-pressure plays a insignificant role for the in-nozzle cavitation patterns when relatively high fuel rail pressures are applied and the cavitation is distinctive [25]. However, the spray emerging from the nozzle bore exit into the spray chamber is heavily affected by the surrounding gas density. Hence, the applied temperature and pressure conditions in this study are not engine-realistic, which is resulting in a not directly comparable spray formation behaviour as in the engine, mostly related to the spray processes following the primary atomization. Nevertheless, highly valuable information of the in-nozzle flow phenomena and its effects on the fuel spray can be obtained.

The fuel used was a standard commercial Diesel from Preem AB (DMK1UA-SE). It has a density of 815.9 kg/m^3, kinematic viscosity of 2.112 mm^2/s and net heat of combustion of 43.16 MJ/kg. The fuel was pressurized using a standard RT-flex common rail system with an injection control unit (ICU) at a rail pressure of 50 MPa. The injection duration was set to 12 ms for all experiments.

2.4. Optical setup

The optical acquisition of the in-nozzle flow using the TNH and the spray morphology of the exiting spray have been simultaneously recorded by setting up two high-speed cameras (Photron Fastcam SA5) with a far-field microscope (Questar QM100) and a zoom lens (Nikon) for the small field of view (FOV) of the in-nozzle flow (approx. 4 × 2.5 mm) and the relatively large FOV of the subsequent spray evolution (approx. 150 × 150 mm), respectively. The FOV of the in-nozzle flow is depicted in Fig. 3 (ii). Two synchronized pulsed diode lasers with a wavelength of 690 ± 10 nm (Cavitar Cavilux Smart) have been used as light sources for the two high-speed cameras. Fig. 4 depicts a schematic of the optical setup for simultaneous acquisition of the in-nozzle flow and spray formation. Note that the fuel injector (1) with the mounted TNH (16) are in proportion and indicate the large size of the fuel injectors used for large two-stroke marine Diesel engines. The line-of-sight optical measurement technique Diffused Back Illumination (DBI) has been applied for both systems [30]. As the two light sources were identical regarding wavelength, the two optical axes were slightly angled (not illustrated in Fig. 4). The miss-alignment however is

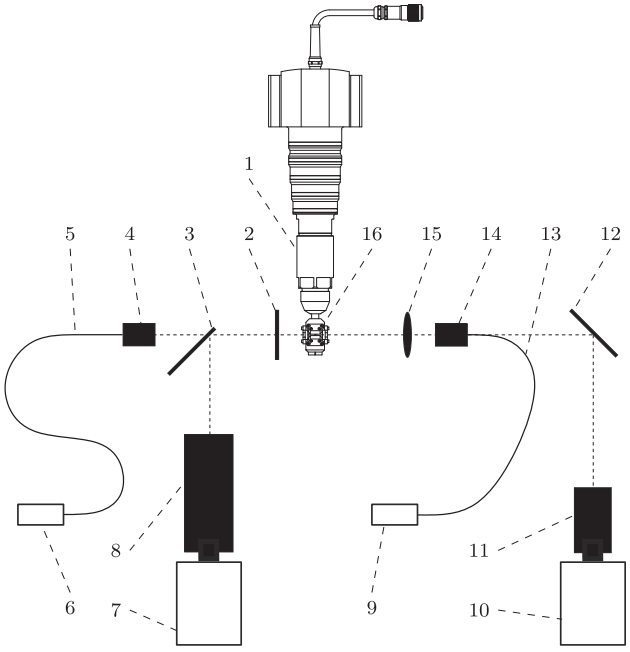

Fig. 4. Schematic of optical setup (diffuse back illumination) for simultaneous acquisition of the in-nozzle flow and spray formation consisting of fuel injector (1), diffuser plate (2), mirror (3, 12), collimator (4, 14), light guide (5, 13), diode laser (6, 9), high-speed camera (7, 10), far-field microscope (8), lens (11), focusing lens (15) and TNH (16).

insignificant as the angle between the two axes was kept very small compared to the distance between cameras and light source. Note that the SCC is not depicted in Fig. 4 for visibility reasons. To focus the light for the in-nozzle flow visualization an additional convex lens (f = 150 mm) has been used (15) behind the collimator (14). A ground glass has been used as diffuser (2) for the spray background illumination. The images were simultaneously acquired at a frame rate of 20 kHz with a resolution of 512 × 512 pixel, i.e. every spray image has the same time stamp as its corresponding in-nozzle flow image. The images acquired have been evaluated using Mathworks Matlab.

3. Results & discussion

3.1. In-nozzle flow

The in-nozzle flow images have been averaged over the quasi-steady-state period of the fuel injection between 6 and 14 ms after triggered start of injection (tSOI) and throughout multiple injections at the same condition. Fig. 5 depicts the averaged in-nozzle flow visualizations with different levels of hydro-erosive grinding of the transparent nozzle and a rail pressure of 50 MPa. Five different levels of hydro-erosive grinding have been investigated together with a sharp-edged, i.e. non hydro-erosive ground, reference atomizer tip (see Table 1). Note that the image of the in-nozzle flow has only been processed by intensity level adjustment/correction, rotation and mapping. The first image in Fig. 5 shows the sharp-edged (reference) orifice without fuel injection (bg), i.e. the nozzle bore is filled with fuel, but as there is no mass flow there is no cavitation. This image serves as background reference. Due to the not perfectly identical refractive indices of PMMA and the Diesel fuel used, the edges of the nozzle bore (vertical) and main bore (horizontal) are still visible as the light is refracted away from the optical axis towards the camera. The other six images (i to vi) in Fig. 5 depict the in-nozzle flow with increasing levels of hydro-erosive grinding towards the right side, i.e. the nozzle in Fig. 5 i) is sharp edged (non hydro-erosive ground) and the nozzle in Fig. 5 vi) is maximally hydro-erosive ground. The level of hydro-erosive grinding could not be extended because the PMMA nozzle failure probability increased significantly after the grinding level of the nozzle vi). The fuel enters the nozzles depicted in Fig. 5 from the left side of the horizontal main bore and enters the nozzle bore from the top side of the images. Dark areas indicate gaseous flow, i.e. cavitation, since the light is refracted off the optical axis, while bright areas, in the limits of the nozzle bore walls, indicate flow of the liquid fuel. As expected, the nozzles without or with less inlet radii due to limited hydro-erosive grinding, show a significantly higher lever of cavitation. The flow patterns for the nozzles depicted in i) to iii) can be clearly characterized as supercavitation [31] since the cavitation emerges over the whole nozzle bore length and reaches the nozzle bore exit. The last three nozzles (iv - vi) have a distinct different cavitation pattern than the previous ones: a strong cavitation swirl motion of the fuel vapour evolves with increasing level of hydro-erosive grinding. This swirl motion is, according to literature, not clearly characterized, but one can argue that it is a combination of string cavitation, cloud cavitation and supercavitation. Fig. 6 presents single shot images of the in-nozzle flow taken at 8 ms after triggered start of injection (tSOI) with the hydro-erosive ground transparent nozzles. Note that the background image with no mass flow as shown in Fig. 5 bg) is not included in Fig. 6 and hence, the labelling in Fig. 6 is kept consistent to ensure comparability between the single shots and averaged images in Fig. 5.

After the cavitation breakup between images (iii) and (iv) in Fig. 6, motion blur appears as the diode laser pulse width and the minimal exposure time of the high-speed camera are too long for the velocities of a couple hundred meters per second in the nozzle bore. This is clearly visible with the slightly drawn-out cavitation patterns. The high fluid velocities and the low acquisition rate of 20 kHz limit the evaluation of quantitative data from the in-nozzle flow images. However, the images

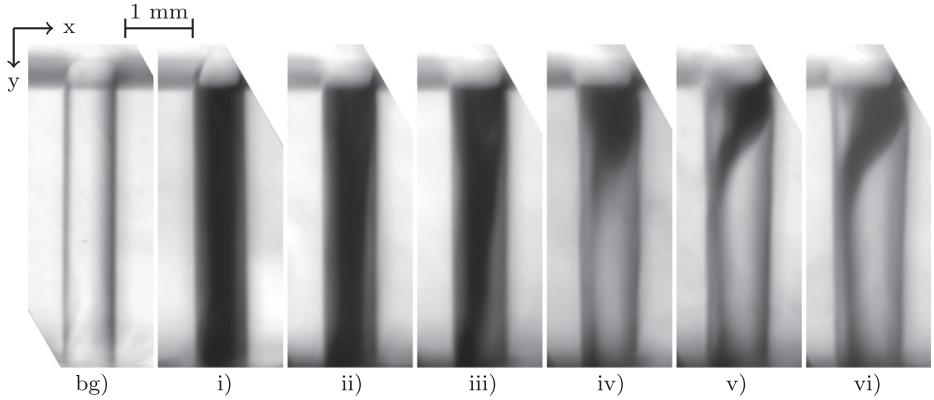

Fig. 5. Background (bg) and averaged in-nozzle flow images during quasi-steady-state fuel injection condition for different levels of hydro-erosive grinding (i - vi) and a rail pressure of 50 MPa. Level of hydro-erosive grinding increases from left to right (i - vi). Dark areas indicate gaseous flow, i.e. cavitation.

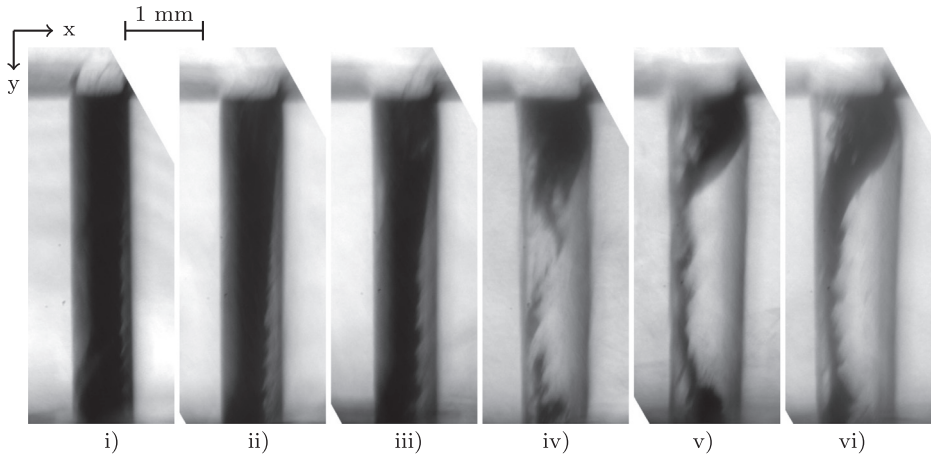

Fig. 6. Single shot in-nozzle flow images at 8 ms after tSOI for different levels of hydro-erosive grinding and a rail pressure of 50 MPa. The hydro-erosive grinding degree increases from left to right (i - vi). Dark areas indicate gaseous flow, i.e. cavitation.

still reveal high-quality qualitative in-nozzle flow cavitation data. The strong swirl motion that evolves with increasing hydro-erosive grinding levels are plausible given the closed geometry of the nozzle main bore (sensor mounted at the end, see Fig. 3) and the eccentricity of the nozzle bore. It also becomes clear from the single shot images in Fig. 6 that the strong swirl motion shapes the geometrical cavitation characteristic in the nozzle bores of the more distinct hydro-erosive ground nozzles (iv -vi). Although hardly visible, the left and right walls of the less hydro-erosive ground nozzles ii) and iii) are cavitation free towards the exit of the orifice, indicating a cavitation pattern similar to the swirl cavitation in nozzles iv) to vi), but more pronounced.

3.2. Fuel injection

The increase of inlet radii through hydro-erosive grinding does not only affect the in-nozzle flow cavitation, but also the pressure measured in the different atomizers. Fig. 7 depicts the measured and averaged fuel pressures of the differently hydro-erosive ground nozzles. The normalized pressure refers to the set rail pressure of 50 MPa and the nomenclature of the different hydro-erosive ground nozzles match the ones in Fig. 5 & 6 and Table 1. It is clearly visible that the sharp-edged nozzle (no HG i) has the steepest pressure rise after the injector needle opening at around 2 ms after triggered start of injection and that the pressure rising gradient decreases with increasing level of hydro-erosive grinding. This can be explained with the reduced flow resistance inside the nozzle tip due to hydro-erosive grinding. The increased nozzle bore diameters and inlet radii between main bore and nozzle hole due to increased levels of hydro-erosive grinding also lead to a different fall time of the pressure after the injector needle closes at around 15 ms after tSOI. The pressure characteristic during the quasi-steady-state fuel injection between around 5 and 15 ms after tSOI remains fairly identical although slightly shifted in x- and y-axis due to delayed pressure build up time and lower static pressure levels with increased level of hydro-erosive grinding. Note that the characteristic injection pressure behaviour is given by the fuel injection system (rail, ICU, fuel pipes, injector, etc.) and is highly reproducible.

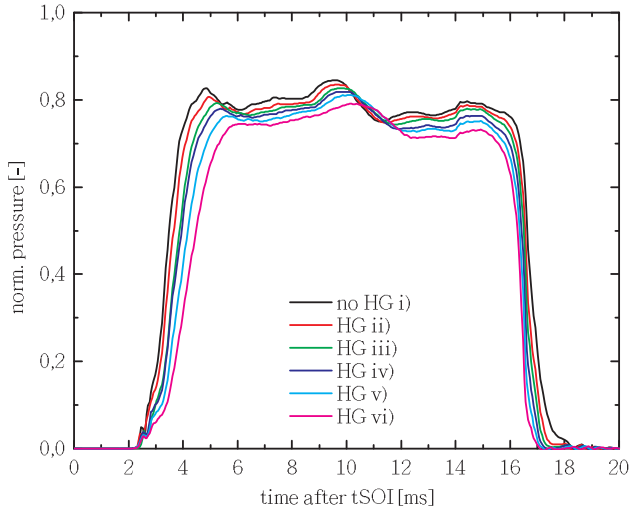

Fig. 7. Averaged fuel pressures measured in the nozzle main bore during injection for different levels of hydro-erosive grinding.

3.3. Spray penetration

Fig. 8 shows the evaluated spray penetration of the six hydro-erosive ground nozzles. The data points have been interpolated and plotted as lines for visibility reasons, but for the sharp-edged nozzle (i), the data points are depicted as well to indicate the high-speed camera frame rate of 20 kHz or 50 μs time steps. The x-axis has been adjusted to the hydraulic start of injection (hSOI) and the spray penetration on the y-axis is limited to 120 mm by the optical access through the windows at the

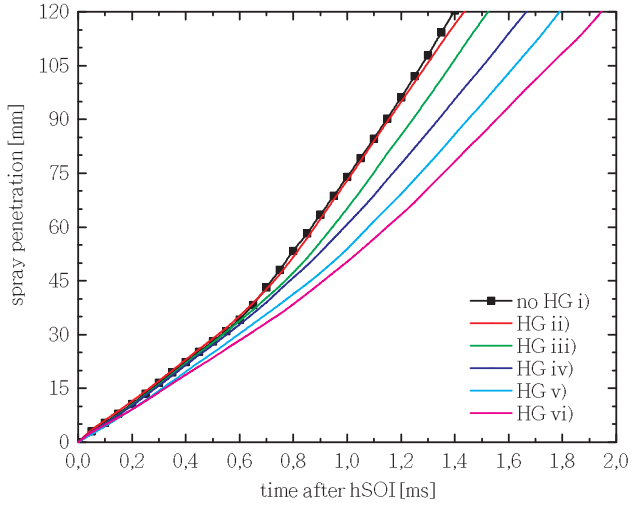

Fig. 8. Spray penetration for the differently hydro-erosive ground nozzles over time after hydraulic start of injection (hSOI). Note that the points depicted for the sharp-edged nozzle (i) indicate the frame rate of 20 kHz of the high-speed camera.

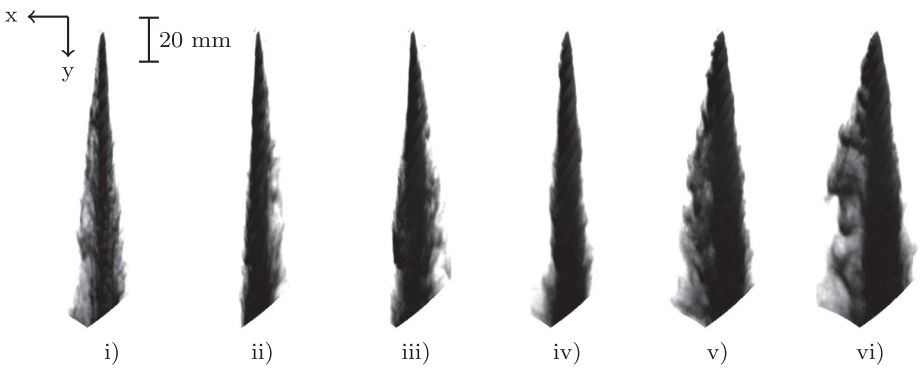

Fig. 9. Single diffused back illuminated spray recordings at 8 ms after triggered start of injection (tSOI) for the differently hydro-erosive ground nozzles (i - vi). Note the vertically flipped coordinate system and the cut-off areas at the bottom due to limited optical access. The nozzle bore exit is at the top of the images and the spray emerges towards the bottom.

SCC. The bend of the penetration curves between around 0.7 ms after hSOI originates from the pressure rise after the injector needle opening. When the two plots in Fig. 7 and 8 are compared, one can see that the fastest pressure rise of the non hydro-erosive ground nozzle (i) also leads to the highest penetration velocity. By increasing the degree of hydro-erosive grinding, the bend in the penetration data extenuates, leading to a significant reduced penetration time of more than 0.5 ms at 120 mm between the non and maximal hydro-erosive ground nozzle (i and vi) or a spray length difference of approximately 52 mm at 1.4 ms after hSOI. However, the data presented in Fig. 8 has to be interpreted with care since the flow resistance and mass flow through the nozzles significantly change with increasing level of hydro-erosive grinding: the nozzle vi) almost doubles the injected amount of fuel compared to the sharp-edged nozzle i) (see Table 1). Furthermore, the spray penetration at ambient gas densities cannot be directly compared to engine relevant conditions with gas densities around 35 kg/m^3.

3.4. Spray morphology

Typical spray images acquired using the line-of-sight optical measurement technique DBI are depicted in Fig. 9. The raw images have been background adjusted to correct inhomogeneities of the illumination. The processed images have then been rotated according to the nozzle bore axis angle and cropped. The shown sprays match the differently hydro-erosive ground nozzles as presented in Fig. 5 & 6. The spray images were acquired 8 ms after triggered start of injection (tSOI) and are therefore matching the time stamp of the in-nozzle flow single shots shown in Fig. 6. The acquired spray images have been evaluated to generate quantitative data to link with the only qualitative in-nozzle flow data available. A threshold has been applied to the processed spray images to separate the spray contour from the background according to [32–35]. The evaluated spray contours have been averaged over the quasi-steady-state fuel injection period and a number of injections and are depicted in Fig. 10. Note that the axes in the plot have different scales and that the standard deviation has not been plotted for visualization purposes. The dashed vertical line represents the geometrical nozzle bore axis and the steps in the contours result from the limited image resolution of only 512 × 512 pixels. With increasing level of hydro-erosive grinding of the eccentric nozzles, the spray disintegrating becomes more unstable. This can be seen in the spray image vi) in Fig. 9 where a higher degree of interaction between spray and ambient gas occurs on the left side of the spray. To visualize the spray contour and its fluctuations, the averaged spray circumference has been plotted together with the standard deviations in Fig. 11. Only the spray contours of the two nozzles (i) and (vi) have been plotted in Fig. 11 for visualization reasons. The averaged spray contours are depicted as solid lines while the according standard deviations are dashed lines. The asymmetrical behaviour of the hydro-erosive ground (vi) in comparison with the sharp-edged (i) spray contour indicate the influence of the in-nozzle cavitation swirl motion on the atomization of the spray. The widening up of the spray angle due to increased atomization caused by

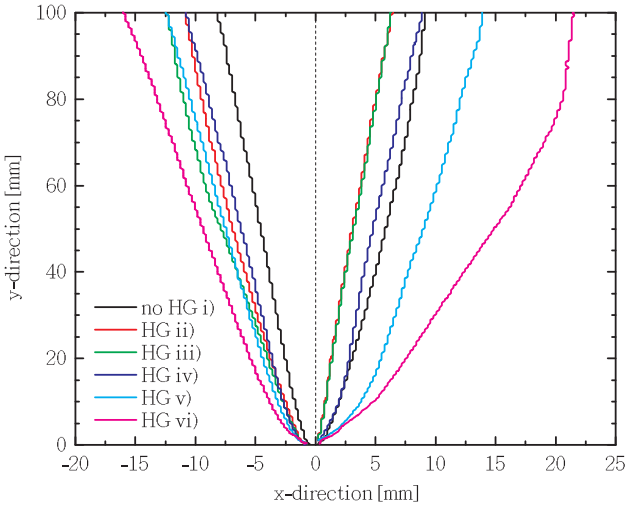

Fig. 10. Averaged spray contours of sprays emerging from nozzles with different levels of hydro-erosive grinding (i - vi). Note that the origin on the x-axis represents the geometrical nozzle bore axis and that the axes have different scales.

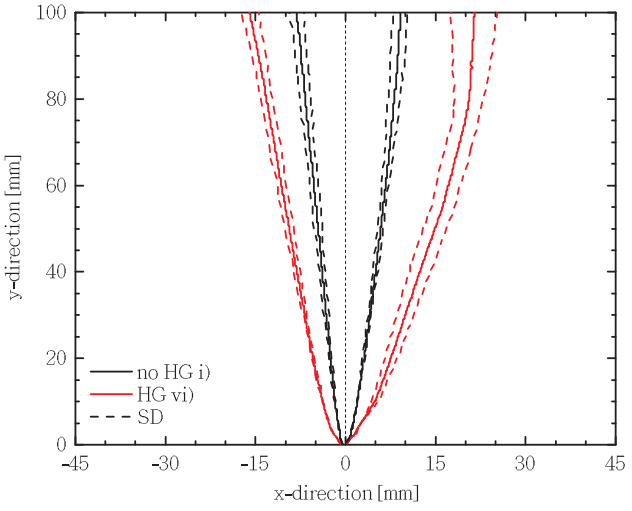

Fig. 11. Averaged spray contour and according standard deviations of sprays emerging from nozzles with sharp-edge, i.e. non (i) and maximal hydro-erosive grinding (vi). Note that the origin on the x-axis represents the geometrical orifice axis and that the axes have different scales.

in-nozzle flow cavitation seems less dominant than the influence of the in-nozzle swirl motion: although the level of geometrical cavitation is clearly reduced with hydro-erosive grinding, the emerging in-nozzle swirl motion significantly enhances the spray widening. In addition, the

swirl motion in combination with the cavitation results in a non-symmetric primary breakup that shows distinctively more instabilities on one side (positive x-axis, see Fig. 11). Although investigated at lower pressures, the spray contours of swirl atomizers show very similar, non-symmetrical shapes affirming the strong swirl motion in the nozzle bores [36].

The standard deviation and hence, the contour fluctuations are significantly larger on the positive x-axis side of the spray. The enhanced atomization leads to a bend in the right sided spray contour in Fig. 11 above around 80 mm from the nozzle bore exit. The data shows that the shape of the spray plume is affected by the location where there is no cavitation at the nozzle bore exit. Larger fuel vortices and fluctuations are present compared to the spray side where the velocity profile and geometrical cavitation occurs remains fairly stable. This direct comparison might be deceptive regarding the existing strong swirl motion of the in-nozzle flow together with the relatively slow image acquisition rate of 20 kHz. Moreover, the optical measurement technique chosen delivers a two-dimensional information and hence, it still can be assumed that the spray fluctuations, although on the different side, are directly triggered by the cavitation at the nozzle bore exit.

The spray angle and axis have been evaluated using the spray contour data of the various nozzles and standard spray morphology analysis methods [33–35]. Fig. 12 shows the spray axis and spray angle of the six nozzles investigated as a function of the mass flow through the nozzles. Note that the increase in mass flow is due to the higher degrees of hydro-erosive grinding of the atomizer: the sharp-edged, i.e. non hydro-erosive ground nozzle (compare with Fig. 5 i) is on the left side of the x-axis around 20 g/s mass flow while the maximal hydro-erosive ground nozzle (compare with Fig. 5 vi) is on the right side at a around 36 g/s (see Table 1). The dashed horizontal line indicates the geometrical axis of the orifice and is set at 0°. The spray angle is massively widening up with increasing level of hydro-erosive grinding as also visible in the averaged spray contours depicted in Fig. 10. By comparing the spray angles in Fig. 12 with the averaged in-nozzle images in Fig. 5 it becomes clear that the spray angle is widening up distinctively after the in-nozzle flow pattern changes between iii) and iv) where the strong cavitation swirl motion appears: the three first nozzles (i - iii) have a very similar spray angle of around 10° while the nozzles (iv), (v) and (vi) widen up distinctively. Compared to the sharp-edged nozzle, the maximal hydro-erosive ground nozzle almost doubles the spray angle. The main reasons for this phenomena are the strong swirl motion of the in-nozzle flow that enhances the spray atomization significantly and the increased nozzle hole diameter due to extensive hydro-erosive grinding.

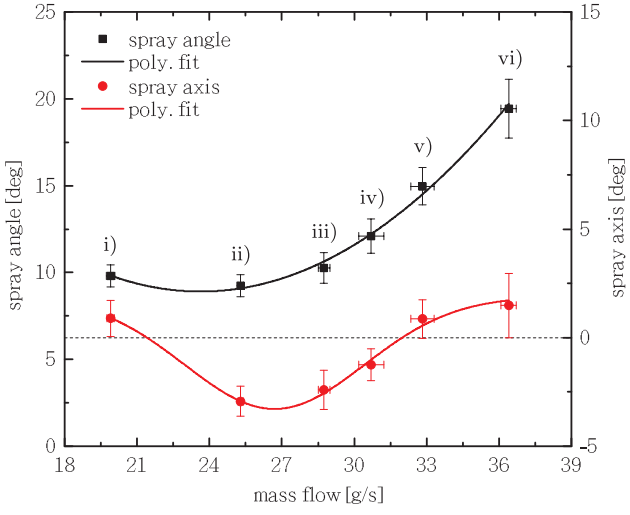

Fig. 12. Spray angle and axis of the differently hydro-erosive ground nozzles (i - vi). The error bars indicate the standard deviations.

However, literature shows that increasing nozzle diameter only slightly increases the spray angle at identical fuel pressures [37] and hence it can be stated that the dominant effect for the widening of the spray is the cavitation swirl motion.

Although the nozzle (i) is supercavitating and has by far the most developed geometrical cavitation pattern, the spray angle remains among the narrowest. Reducing cavitation with a first level of hydro-erosive grinding shows a small decrease in spray angle (ii) which is in agreement with literature that indicates narrower spray angle with less in-nozzle flow cavitation [18,38–40]. However, after a certain amount of hydro-erosive grinding (iii -iv), where the cavitation pattern suddenly changes (compare with in-nozzle flow images in Fig. 5) from slightly diverted supercavitation to swirl cavitation, the increase in spray angle strongly ascends. Such a strong spray angle increase due to string cavitation which describes the here presented cavitation phenomena the best, has also been reported by [39,23]. The axis of the spray behaves differently. While the sharped-edge nozzle (i) is already off-axis (compare with horizontal dashed line at 0°), increasing the level of hydro-erosive grinding first changes the axis to the negative (compare with coordinate systems depicted in Fig. 3). While further hydro-erosive grinding returns the axis towards the geometrical origin. The increased vertical error bars of the nozzle vi) also indicate the strong fluctuation of the spray contour during the quasi-steady-state fuel injection which can be seen on the spray images in Fig. 9 and the spray contour plot showing the standard deviation in Fig. 11.

The spray evolution during start of hydraulic injection for the differently hydro-erosive ground nozzles is shown in Fig. 13. The spray develops from the left to the right side where a quasi-steady-state condition is reached (compare with enlarged, single spray images in Fig. 9). The Figure shows 40 single spray images per nozzle (i - vi) with a time-step of 50 μs, showing a time series between 0 and 2 ms after start of hydraulic injection. The developed sprays on the right side are cut-off due to limited optical access. The spray angle behaviour of first narrowing and then widening up with increasing level of hydro-erosive grinding (i - vi) is already visible during the transient spray evolution (compare with data in Fig. 12).

Due to the limiting thermal durability of the transparent nozzles, the influence of the cavitation could not be linked to the combustion which plays an enormous role on engine efficiency and emissions. However, the investigations of the non-reactive sprays show significant influence of the in-nozzle flow cavitation and hence directly indicate a strong influence on the combustion process since spray atomization and spray combustion are heavily interdependent. The newfound swirl cavitation pattern enhances the spray atomization significantly and allows to design better nozzles with defined cavitation patterns to increase the engines thermal efficiency by improving the spray breakup and the subsequent combustion process.

4. Conclusions

The in-nozzle flow visualizations show a highly dominant role of cavitation regarding the injection processes of large two-stroke marine Diesel engines. Even an extensive level of hydro-erosive grinding of the nozzles cannot completely remove cavitation effects investigated with nozzle tips of relevant geometrical dimensions and applied injection pressures. However, the degree of geometrical cavitation can clearly be reduced through widening up of the nozzle bore and increasing the inlet radii between main bore and nozzle bore through hydro-erosive grinding.

Through the eccentrical arrangement of the nozzle bore, a specific cavitation swirl pattern occurs at higher levels of hydro-erosive grinding. This composition between geometrical and string cavitation leads to one-sided spray contour fluctuations that affect the emerging spray significantly. The spray angle increases with increasing level of hydro-erosive grinding and resulting level of cavitation swirl pattern. The simultaneous acquisition of in-nozzle flow and spray images reveals

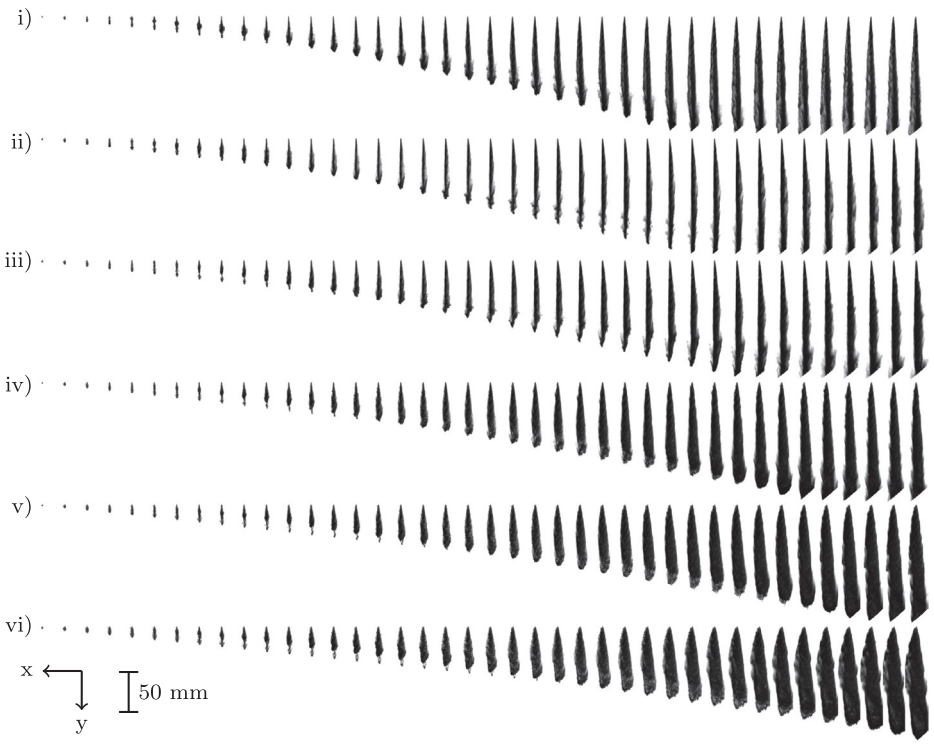

Fig. 13. Diffused back illuminated spray evolution during start of hydraulic injection for the differently hydro-erosive ground nozzles (i - vi). The time step between the single spray images is 50 μs (20 kHz frame rate) and the spray evolves towards the negative x axis.

that the spray fluctuations occur on the side where the in-nozzle images indicate no cavitation. However, due to the strong swirl motion given by the eccentric arrangement of the nozzle bore and the limited image acquisition resolution in time and space it seems more likely that the cavitation at the nozzle bore exit is responsible for the one-sided spray fluctuations.

The experiments have also shown that measuring the fuel pressure in the nozzle main bore allows to characterize the nozzle flow accurately, especially by evaluating the pressure rise and fall times after the needle movement of the injector.

Declaration of Competing Interest

The authors declare that they have no known competing financial interests or personal relationships that could have appeared to influence the work reported in this paper.

Acknowledgments

The authors would like to thank the Combustion Engine Research Center (CERC) affiliated to Chalmers University of Technology, the Swedish Energy Agency and the Swiss Federal Office of Energy for financial support.

References

[1] UNCTAD, Review of Maritime Transport 2016, Technical Report, 2016. URL: http://unctad.org/en/PublicationsLibrary/rmt2016_en.pdf.
[2] M. Linne, Imaging in the optically dense regions of a spray: a review of developing techniques, Prog. Energy Combust. Sci. 39 (2013).
[3] Z. Wang, X. Dai, F. Liu, Z. Li, H. Wu, Breakup of fuel sprays under cavitating and flash boiling conditions, Appl. Therm. Eng. 143 (2018).
[4] F. Liu, Z. Li, Z. Wang, X. Dai, C.F. Lee, Dynamics and primary breakup of cavitation bubbles under throttling conditions, Appl. Therm. Eng. 149 (2019).
[5] A. Schmid, B. von Rotz, R. Schulz, K. Herrmann, G. Weisser, R. Bombach, Influence of nozzle hole eccentricity on spray morphology, in: ILASS - Europe, 25th European Conference on Liquid Atomization and Spray Systems, Chania, Greece, 2013.
[6] I. Nagy, A. Schmid, S. Hensel, C. Dahnz, Computational analysis of spray primary breakup in 2-stroke marine diesel engines with different nozzle layouts, in: ICLASS - 13th Triennial International Conference on Liquid Atomization and Spray Systems, Tainan, Taiwan, 2015.
[7] I. Nagy, A. Matrisciano, H. Lehtiniemi, F. Mauss, A. Schmid, Influence of Nozzle Eccentricity on Spray Structures in Marine Diesel Sprays, SAE Tech. Paper Ser. 1 (2017).
[8] A. Schmid, C. Habchi, J. Bohbot, B. von Rotz, K. Herrmann, R. Bombach, G. Weisser, Influence of in-nozzle flow on spray morphology, in: ILASS - Europe, 26th European Conference on Liquid Atomization and Spray Systems, Bremen, Germany, 2014.
[9] S. Martynov, D. Mason, M.R. Heikal, S.S. Sazhin, M. Gorokhovski, Modelling of Cavitation Flow in a Nozzle and Its Effect on Spray Development, International Heat Transfer Conference 13, Sydney, Australia, 2006.
[10] Y. Sun, Z. Guan, K. Hooman, Cavitation in Diesel Fuel Injector Nozzles and its Influence on Atomization and Spray, Chem. Eng. Technol. 42 (2019).
[11] F. Payri, V. Bermúdez, R. Payri, F.J. Salvador, The influence of cavitation on the internal flow and the spray characteristics in diesel injection nozzles, Fuel 83 (2004).
[12] M. Mirshahi, J. Nouri, Y. Yan, M. Gavaises, Link between in-nozzle cavitation and jet spray in a gasoline multi-hole injector, ILASS - Europe, 25th European Conference on Liquid Atomization and Spray Systems, Chania, Greece, 2013.
[13] M. Shervani-Tabar, S. Parsa, M. Ghorbani, Numerical study on the effect of the cavitation phenomenon on the characteristics of fuel spray, Math. Comput. Model. 56 (2012).
[14] X. Wu, J. Deng, H. Cui, F. Xue, L. Zhou, F. Luo, Numerical simulation of injection rate of each nozzle hole of multi-hole diesel injector, Appl. Therm. Eng. 108 (2016).
[15] L. Lešnik, B. Kegl, G. Bombek, M. Hočevar, I. Biluš, The influence of in-nozzle cavitation on flow characteristics and spray break-up, Fuel 222 (2018).
[16] E. Hutli, M. Nedeljkovic, A. Bonyár, D. Légrády, Experimental study on the influence of geometrical parameters on the cavitation erosion characteristics of high speed submerged jets, Exp. Thermal Fluid Sci. 80 (2017).
[17] Z. Falgout, M. Linne, Novel design for transparent high-pressure fuel injector nozzles, Rev. Sci. Instrum. 87 (2016).
[18] M. Blessing, G. König, C. Krüger, U. Michels, V. Schwarz, Analysis of flow and cavitation phenomena in diesel injection nozzles and its effects on spray and mixture formation, SAE Tech. Paper 01–1358 (2003).
[19] Z. Falgout, M. Linne, Design Method for Optically Transmissive Nozzles for High-Pressure Experimental Fuel Injectors, in: ILASS - Americas, 27th Annual Conference on Liquid Atomization and Spray Systems, Raleigh, NC, USA, 2015.
[20] T. Qiu, X. Song, Y. Lei, X. Liu, X. An, M. Lai, Influence of inlet pressure on cavitation flow in diesel nozzle, Appl. Therm. Eng. 109 (2016).
[21] Z. Chen, A. Yao, C. Yao, Z. Yin, H. Xu, P. Geng, Z. Dou, J. Hu, T. Wu, M. Ma, Effect of fuel temperature on the methanol spray and nozzle internal flow, Appl. Therm. Eng. 114 (2017).
[22] W. Yu, W. Yang, F. Zhao, Investigation of internal nozzle flow, spray and combustion characteristics fueled with diesel, gasoline and wide distillation fuel (WDF) based on a piezoelectric injector and a direct injection compression ignition engine, Appl. Therm. Eng. 114 (2017).
[23] T. Cao, Z. He, H. Zhou, W. Guan, L. Zhang, Q. Wang, Experimental study on the effect of vortex cavitation in scaled-up diesel injector nozzles and spray characteristics, Exp. Therm. Fluid Sci. 113 (2020).

[24] B. Kim, S. Park, Study on in-nozzle flow and spray behavior characteristics under various needle positions and length-to-width ratios of nozzle orifice using a transparent acrylic nozzle, Int. J. Heat Mass Transf. 143 (2019).
[25] R. Balz, A. Schmid, D. Sedarsky, Cavitation flow visualization in marine diesel injectors, COMODIA - 9th International Conference on Modeling and Diagnostics for Advanved Engine Systems, Okayama, Japan, 2017.
[26] R. Balz, A. Schmid, D. Sedarsky, In-Nozzle Flow Visualization of Marine Diesel Injector Nozzles with Different Inlet Radii, International Cavitation Symposium, Baltimore, MD, USA, 2018.
[27] K. Herrmann, Development of a reference experiment for large diesel engine combustion system optimization, in: CIMAC Congress, Vienna, Austria, 2007.
[28] K. Herrmann, B. von Rotz, R. Schulz, G. Weisser, B. Schneider, K. Boulouchos, A spray combustion chamber facility for investigations in relation to large 2-stroke marine diesel engine combustion system optimization, ISME - Proceedings of the International Symposium on Marine Engineering, Kobe, Japan, 2011.
[29] R. Balz, D. Sedarsky, Temperature Dependent In-Nozzle Flow Investigations of Marine Diesel Injectors, ILASS - Americas, 30th Annual Conference on Liquid Atomization and Spray Systems, Tempe, AZ, USA, 2019.
[30] J. Du, B. Mohan, J. Sim, W.L. Roberts, Experimental study on the non-reacting spray characterization of gasoline compression ignition fuel, Energy Proc. 158 (2019).
[31] M. Jeshani, Optical characterisation of cavitating flows in diesel fuel injection equipment, Ph.D. thesis, City University London, 2013.
[32] R. Payri, J. Gimeno, G. Bracho, D. Vaquerizo, Study of liquid and vapor phase behavior on Diesel sprays for heavy duty engine nozzles, Appl. Therm. Eng. 107 (2016).
[33] R. Payri, F.J. Salvador, P. Martí-Aldaraví, D. Vaquerizo, ECN Spray G external spray visualization and spray collapse description through penetration and morphology analysis, Appl. Therm. Eng. 112 (2017).
[34] C. Tang, Z. Feng, C. Zhan, W. Ma, Z. Huang, Experimental study on the effect of injector nozzle K factor on the spray characteristics in a constant volume chamber: Near nozzle spray initiation, the macroscopic and the droplet statistics, Fuel 202 (2017).
[35] Y. Lei, J. Liu, T. Qiu, J. Mi, X. Liu, N. Zhao, G. Peng, Effect of injection dynamic behavior on fuel spray penetration of common-rail injector, Energy 188 (2019).
[36] J. Cui, H. Lai, J. Li, Y. Ma, Visualization of internal flow and the effect of orifice geometry on the characteristics of spray and flow field in pressure-swirl atomizers, Appl. Therm. Eng. 127 (2017).
[37] S.J.M. Algayyim, A.P. Wandel, T. Yusaf, The impact of injector hole diameter on spray behaviour for butanol-diesel blends, Energies 11 (2018).
[38] H. Suh, C. Lee, Effect of cavitation in nozzle orifice on the diesel fuel atomization characteristics, Int. J. Heat Fluid Flow 29 (2008).
[39] T. Hayashi, M. Suzuki, M. Ikemoto, Visualization of Internal Flow and Spray Combustion with Real Size Diesel Nozzle, Trans. Soc. Autom. Eng. Japan 43 (2012).
[40] B. Abderrezzak, Y. Huang, Investigation of the effect of cavitation in nozzles with different length to diameter ratios on atomization of a liquid jet, J. Therm. Sci. Eng. Appl. 9 (2017).